Supporting Information

Efficient ternary organic photovoltaic device with a non-halogenated solvent *via* synergistic inhibiting charge recombination and regulating morphology

Xingpeng Liu,[a, b] Yichun Peng,[c, d *] Zezhou Liang,[e] Limin Wang,[a] Shenghui Han,[a] Zheng Dou,[a] Xubin Lu,[a] Junfeng Tong,[a] Jiangang Liu [b *] and Jianfeng Li[a *]

[a]School of Materials Science and Engineering, Lanzhou Jiaotong University, Lanzhou, 730070, China.

[b] School of Electronics and Information, Northwestern Polytechnical University, Xi'an, 710129, China

[c]School of Civil Engineering, Lanzhou Institute of Technology, Lanzhou, 730050, China.

[d]Key Laboratory of Optoelectronic Chemical Materials and Devices (Ministry of Education), School of Optoelectronic Materials & Technology, Jianghan University, Wuhan, 430056, China

[e]Key Laboratory for Physical Electronics and Devices of the Ministry of Education & Shaanxi Key Lab of Information Photonic Technique, School of Electronics and Information Engineering, Xi'an Jiaotong University, Xi'an, 710049, China.

Corresponding Author:

E-mail: yichunpeng77@163.com (Y. Peng)

E-mail: jgliu@nwpu.edu.cn (J.Liu)

E-mail: ljfpyc@163.com (J. Li)

Device Fabrication

OPV devices were fabricated with a conventional structure ITO/PEDOT:PSS/active layers/PDINO/Al. The PEDOT:PSS solutions were spin coated on the pre-cleaned ITO glass substrates with a spin rate of 4400 rpm for 30 s and then annealed on a hot plate at 150 ℃ for 15 min in air to obtain uniform films. The substrate was transferred to a glove box filled with N_2 and used to prepare the active layer. The active layer solutions were prepared in *o*-xylene (*o*-XY) (with an acceptor concentration of 10 mg mL^{-1} and a D/A ratio at 1:1), The 1vol% diphenyl sulfide (DPS) was added in the blend solution before spin-coat on the PEDOT:PSS films and continuously stirred for 30 min. The blend solutions were spin-coated onto the ITO/PEDOT:PSS substrates at 1800 rpm for 30 s to obtain approximately 110 nm thick active layer. The active layers on the substrate were annealed at 110 ℃ for 10 min. After that, PDINO solution (1 mg·mL^{-1} in methanol) was spin-coated on the top of active lavers at 3000 rpm for 30 s to prepare cathode interlayer. Finally, the cathode of Al was deposited by thermal evaporation with a shadow mask under 10^{-4} Pa.

Instruments and Measurements

The current density-voltage (*J-V*) characteristics of the solar cells were performed using a programmable Keithley 2400 source measurement unit under simulated solar light (AM 1.5G). External quantum efficiencies (EQEs) were measured using an incident photon-to-charge carrier efficiency (IPCE) setup (7-SCSpeclII, Beijing 7-star Optical Instruments Co.) equipped with a standard Si diode. The ultraviolet-visible (UV-visible) absorption spectra were recorded on a UV-1800 spectrophotometer (Shimadzu, Kyoto, Japan). The morphology of the films were characterized by a tapping-mode atomic force microscope (AFM, Agilent 5400). Grazing incidence wide-angle X-ray scattering (GIWAXS) patterns were acquired by beamline BL16B1 (Shanghai Synchrotron Radiation Facility). The X-ray wavelength was 0.124 nm (E=10 keV), and the incidence angle was set to 0.2°.

SCLC Mobility Measurements

Hole-only and electron-only devices were fabricated with device structure of ITO/PEDOT:PSS/Active layer/MoO_3/Ag and ITO/ZnO/Active layer/PDINO/Al, respectively. The Mott-Gurney law was used to calculate the mobilities of hole (μ_h) and electron (μ_e) in the binary and ternary devices, respectively, and the corresponding results are estimated using the following equation:

$$J = \frac{9}{8}\varepsilon_0\varepsilon_r\mu\frac{V}{L^3} \quad (1)$$

where ε_r refers to the dielectric constant of the material, ε_0 stands for the vacuum dielectric constant, μ is the charge mobility, $V = V_{appl}-V_{bi}$ (where V_{appl} is the applied voltage; V is the built-in electric field of the device, which has a value of about 0.1 V), and L (=110 nm) is the thickness of the active layer.

TPV and TPC

TPV was testing under the open-circuit condition to explore the photovoltage decay. The subsequent voltage decay is then recorded by the digital storage oscilloscope to directly monitor non-geminate charge carrier recombination. The intensity of light is 230 $\mu W \cdot cm^{-2}$ and the wavelength of light is 520 nm and the light pulse is 10 ns. The normalized curves are easier to compare the carrier lifetime and the slow decline one is the one with a long lifetime. TPC was testing under the short-circuit condition to explore the time-dependent extraction of photogenerated charge carriers. The 10 ns light plus laser were selected to the light source for steady the photogenerated current density. The devices are otherwise kept in the dark between pulses in order to avoid any influence of pulse frequency on the current responses.

Femtosecond Transient Absorption (fs-TA) Measurements

Fs-TA spectroscopy was performed to measure the temporal evolution of the absorption changes in the excited states, through which the carrier dynamics in femtosecond to nanosecond regime could be revealed. The laser beam is supplied by amplified Ti: sapphire laser source (800 nm, Coherent) that provides 100 fs pulses with

a repetition rate of 1 kHz. The output was split into two beams, the stronger one of which was frequency doubled to generate a 400 nm pump light, and the other one was focused into a sapphire plate to generate a broadband supercontinuum probe light. Using an optical chopper, the repetition rate of the pump pulses were adjusted to 500 Hz, and were focused on the sample with the probe pulse (white light). The TA spectra were obtained by comparing the probe light spectra with and without pump light excitation. The photoinduced absorption change as a function of wavelength was described using optical density (absorbance) changes. By adjusting the delay time between the pump and probe pulses, a 3D transient spectral image was formed.

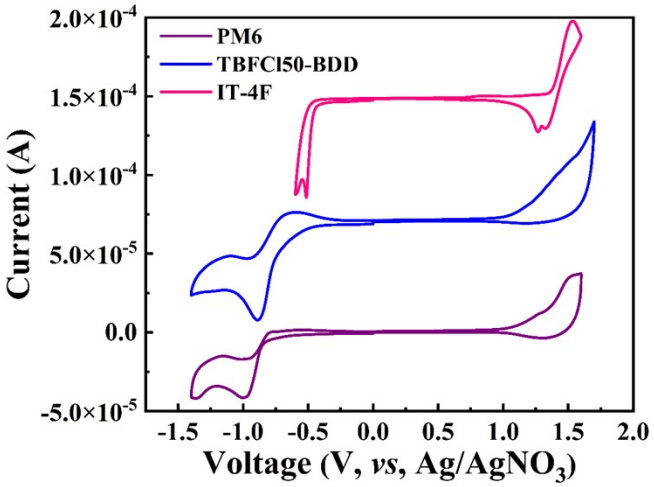

Figure S1. CV curves of PM6, TBFCl50-BDD and IT-4F.

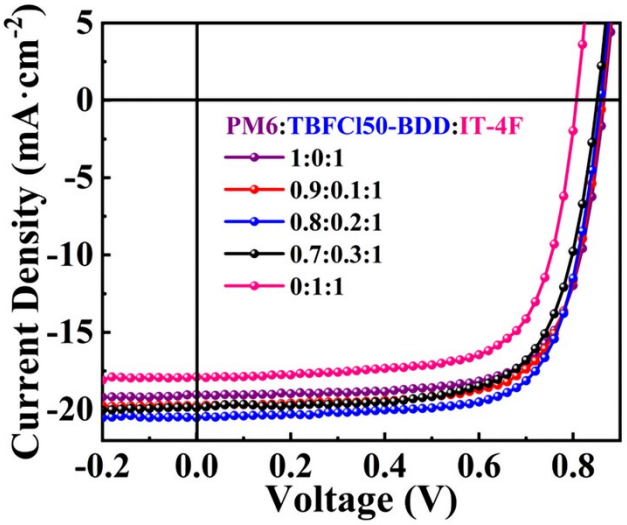

Figure S2. *J-V* curves of binary and ternary OPV devices.

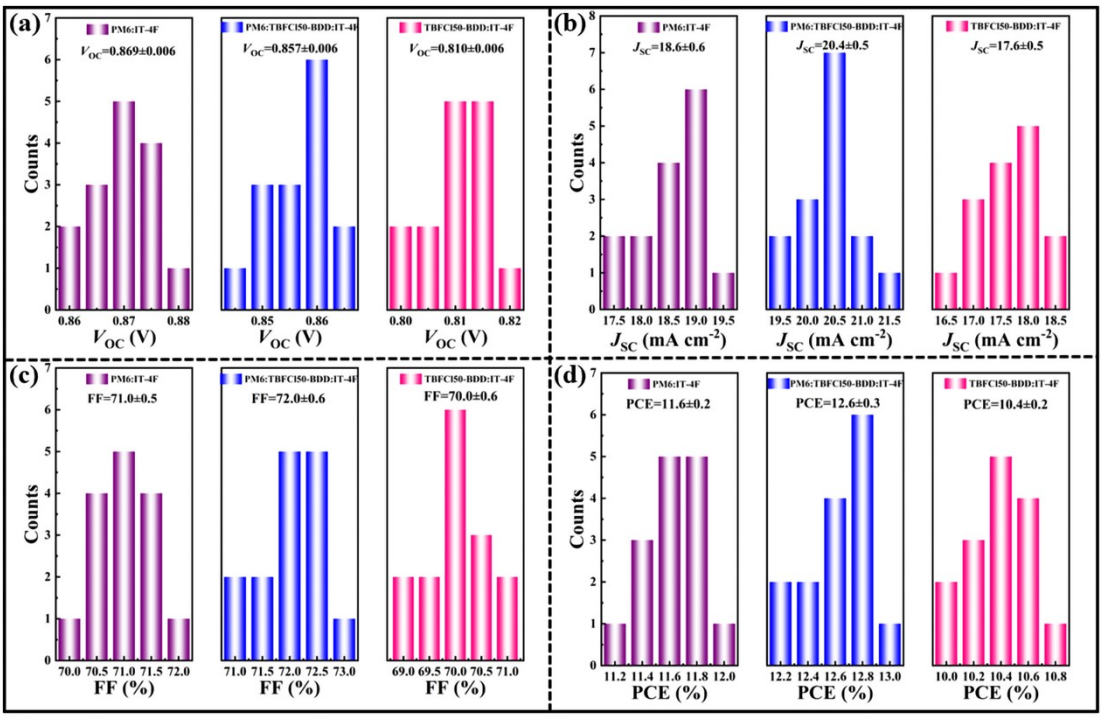

Figure S3. Histograms of device parameters (J_{SC}, V_{OC}, FF and PCE) for binary and ternary devices.

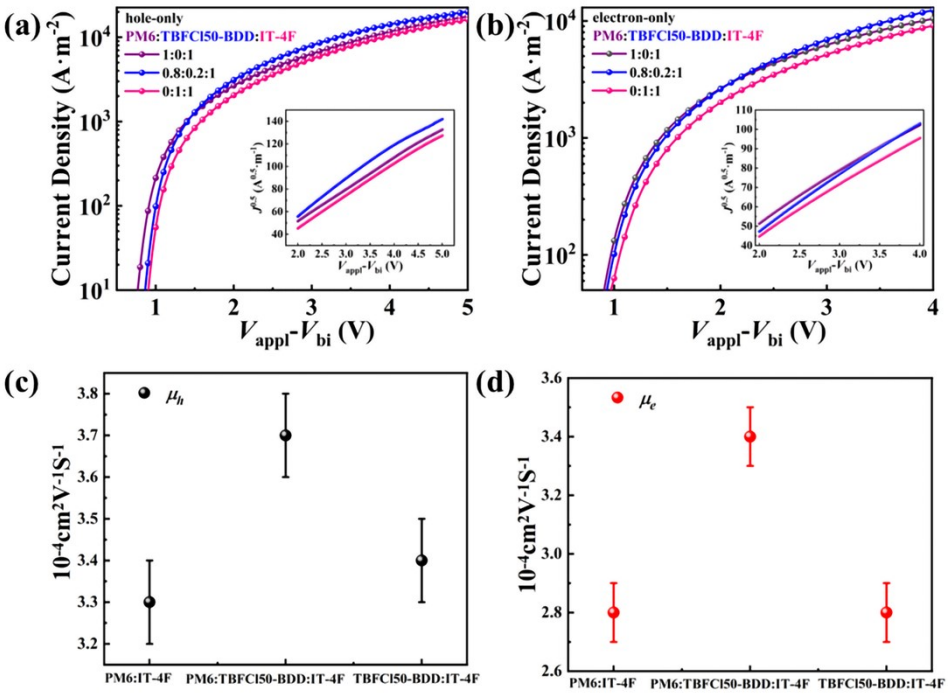

Figure S4. (a) Hole mobilities and (b) electron mobilities for binary and ternary devices. The mobility values of (c) hole-only and (d) electron-only devices.

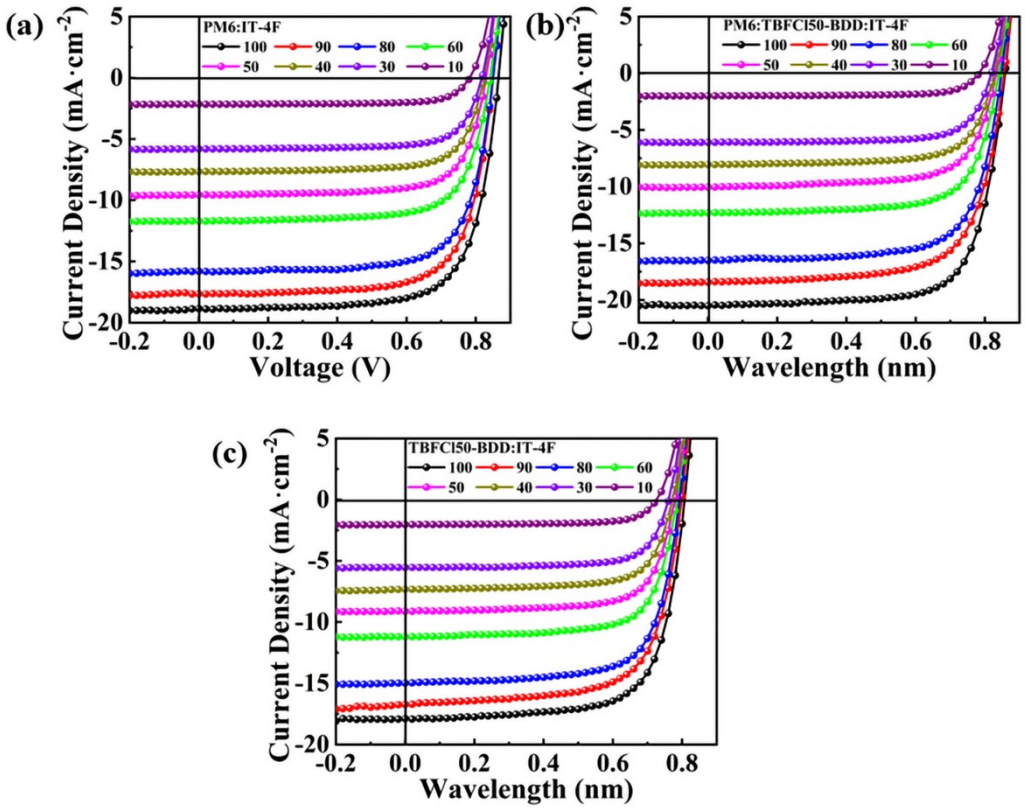

Figure S5. *J-V* curves with various incident light intensities of (a) PM6:IT-4F (b) PM6:TBFCl50-BDD:IT-4F, and (c) TBFCl50-BDD:IT-4F devices.

Table S1. The electrochemical properties of polymers PM6, TBFCl50-BDD and IT-4F.

Materials	φ_{ox}^{onset} (eV)	φ_{red}^{onset} (eV)	E_{HOMO}[a] (eV)	E_{LUMO}[b] (eV)
PM6	1.06	-0.83	-5.43	-3.54
TBFCl50-BDD	1.10	-0.67	-5.47	-3.70
IT-4F	1.37	-0.45	-5.74	-3.92

[a] Calculated by $E_{HOMO} = -e(\varphi_{ox}^{onset} + 4.37)eV$, [b] Calculated by $E_{LUMO} = -e(\varphi_{red}^{onset} + 4.37)eV$

Table S2. Photovoltaic performance of binary and ternary OPV devices.

PM6:TBFCl50-BDD:IT-4F	V_{OC} (V)	J_{SC} (mA cm^{-2})	FF (%)	PCE[a] (%)
1:0:1	0.870 (0.869±0.006)	19.0 (18.6±0.6)	71.4 (71.0±0.5)	11.8 (11.6±0.2)
0.9:0.1:1	0.863 (0.862±0.006)	19.8 (19.4±0.5)	71.7 (71.5±0.5)	12.2 (11.9±0.3)
0.8:0.2:1	0.858 (0.857±0.006)	20.6 (20.4±0.5)	72.4 (72.0±0.6)	12.8 (12.6±0.3)
0.7:0.3:1	0.850 (0.845±0.006)	19.9 (19.5±0.6)	70.6 (70.3±0.5)	11.93 (11.60±0.2)
0:1:1	0.812 (0.807±0.006)	18.1 (17.6±0.5)	70.5 (70.0±0.6)	10.4 (10.4±0.2)

[a] Average values from 15 devices.

Table S3. Exciton dissociation rates, exciton collection rates and maximum exciton generation rates binary and ternary device

PM6:TBFCl50-BDD:IT-4F	J^*_{ph}[a] (mA cm^{-2})	$J^{\#}_{ph}$[b] (mA cm^{-2})	J_{sat}[c] (mA cm^{-2})	η_{diss}[d] (%)	η_{coll}[e] (%)	G_{max}[f] (m^3 s^{-1})
1:1:0	18.85	16.25	19.67	95.83	82.61	1.23×10^{28}
0.8:0.2:1	20.49	18.12	21.09	97.16	85.92	1.32×10^{28}
0:1: 1	17.84	15.04	18.68	95.50	80.51	1.17×10^{28}

[a] J_{ph}^* refers to the current density under the short circuit condition; [b] $J_{ph}^{\#}$ is the current density under the maximum power output condition; [c] $J_{sat} = qLG_{max}$, J_{sat} represents the saturation photocurrent density; [d] $\eta_{diss} = J_{ph}^*/J_{sat}$; [e] $\eta_{coll} = J_{ph}^{\#}/J_{sat}$; [f] G_{max} is the maximum exciton generation rate.

Table S4. Hole mobility, electron mobility and their ratios for PM6:IT-4F, PM6:TBFCl50-BDD:IT-4F and TBFCl50-BDD:IT-4F binary and ternary devices

PM6:TBFCl50-BDD:IT-4F	μ_h ($\times10^{-4}$cm^{2}V^{-1}s^{-1})	μ_e ($\times10^{-4}$cm^{2}V^{-1}s^{-1})	μ_h/μ_e
1:0:1	3.3	2.8	1.2
0.8:0.2:1	3.7	3.4	1.1
0:1:1	3.4	2.8	1.2

Table S5. Contact angle and surface energy parameters for PM6, TBFCl50-BDD and IT-4F.

Materials	Water (°)	Ethylene glycol (°)	γ (mN m^{-1})
PM6	111.2	85.5	21.46
TBFCl50-BDD	113.4	84.1	23.56
IT-4F	94.5	66.2	28.90